RAM is upregulated during T cell activation and is required for RNA cap formation and gene expression

Katarzyna Knop[1,2*], Carolina Gomez-Moreira[2*], Alison Galloway[1,2], Dimitrinka Ditsova[1,2] and Victoria H Cowling[1,2,3*]

[1]Cancer Research UK Scotland Institute, Glasgow, G61 1BD, U.K.

[2]School of Life Sciences, University of Dundee, Dundee, DD1 5EH, U.K.

[3]School of Cancer Sciences, University of Glasgow, Glasgow, G61 1QH, U.K.

*Corresponding author

Victoria.cowling@glasgow.ac.uk

Katarzyna Knop and Carolina Gomez Moreira are co-first author

Abstract

On T cell activation, upregulation of gene expression produces the protein required for the differentiation and proliferation of effector cell populations. RAM, the co-factor of the RNA cap methyltransferase RNMT, is upregulated following activation. Formation of the RNA cap protects RNA during synthesis and guides RNA processing and translation. Using conditional gene deletion, we found that *Ram* expression stabilises RNMT protein in T cells and is required for its upregulation on activation. When the *Ram* gene is deleted in naïve T cells, there are major impacts on activation-induced RNA cap formation and gene expression. Activated T cell proliferation is dependent on increased ribosome production; in *Ram* knock-out T cells activation-induced expression of ribosomal protein genes and snoRNAs is most severely reduced. Consistent with these changes, *Ram* deletion resulted in reduced protein synthesis, and reduced growth and proliferation of CD4 T cells. Deletion of *Ram* results in a similar but milder phenotype to *Rnmt* deletion, supporting the role of RAM as a RNMT co-factor.

Keywords:

Abbreviations:

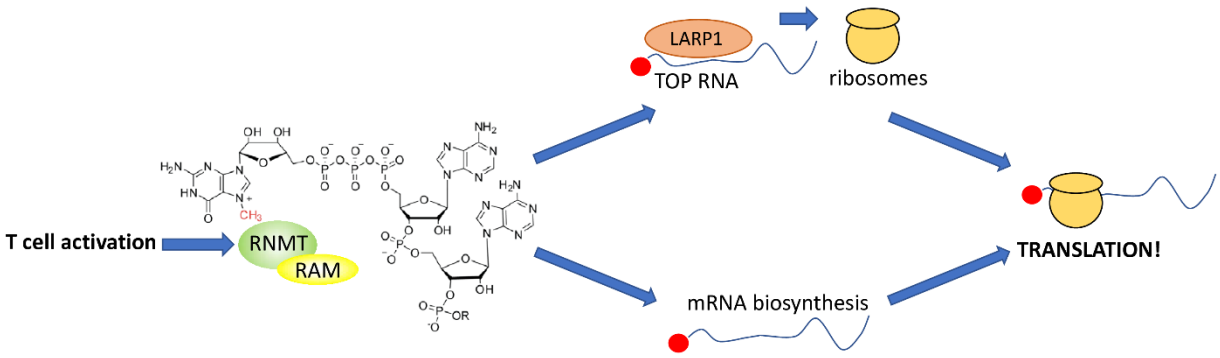

Graphical Abstract: Following T cell activation, the RNA cap methyltransferase RNMT-RAM is upregulated which results in increased RNA cap formation. The RNA cap protects mRNA and other RNA pol II-transcribed RNAs during synthesis and recruits factors involved in RNA processing and translation. During T cell activation, upregulation of RNMT-RAM is required for upregulation of mRNA biosynthesis and the enhanced production of TOP-RNAs (via a LARP1 interaction), which drives ribosome production. Overall, following T cell activation, RNMT-RAM upregulation facilitates the production of the mRNA and the ribosomes required for rapid translation and cell proliferation.

Introduction

When T cells are activated in response to antigen recognition, elevated transcription, RNA processing and translation accelerate the protein production required for rapid proliferation and differentiation into effector lineages (1-4). During this phase of rapid gene expression, increased RNA cap formation on RNA pol II transcripts is critical (5). The RNA cap protects RNA during transcription and recruits factors involved in RNA processing, export and translation (6, 7). Upregulation of the major RNA cap methyltransferase, RNMT (RNA guanosine N-7 cap methyltransferase), is required for increasing gene expression in activated T cells (5).

RNMT increases mRNA production via co- and post-transcriptional stabilisation of RNA and via non-catalytic impacts on mRNA production (5, 7-9). A key function of the RNA cap is to mediate recruitment of mRNA to the ribosome. In T cells, RNMT additionally increases the ribosome content. RNMT has specific impacts on ribosome production by selectively upregulating RNAs encoding ribosomal proteins, ribosomal RNA synthesis and processing factors, and ribosome biogenesis factors (5). Many RNAs governing ribosome production or translation are members of the TOP RNA family, which have a 5' polypyrimidine tract that binds to the RNA cap binding protein LARP1 (La Ribonucleoprotein 1, Translational Regulator), which protects RNA from degradation and impacts on translation (10, 11). *In vitro*, RNMT catalysed N-7 cap guanosine methylation is required for LARP1 to interact with capped RNA and in T cells LARP1-interacting RNAs are repressed following *Rnmt* gene deletion (5, 12-14). Thus the LARP1-m7G interaction selectively enhances the stability of TOP-RNAs during T cell activation, providing the increased ribosome content required for RNA translation and cell proliferation.

The expression and activity of RNMT is dependent on its co-factor RAM (RNA-activating mini protein/RAMAC)(15). RAM has several positive impacts on RNMT function; RAM binding to RNMT alters active site dynamics resulting in increased RNA cap methylation, RAM has a RNA binding domain which recruits RNA to the RNMT complex, and RAM increases the stability of RNMT (8, 15-18). During embryonic stem cell differentiation, regulation of RAM has a critical role (19, 20). RAM is repressed during embryonic stem cell differentiation resulting in reduced RNMT activity; this mechanism is necessary for repression of pluripotency genes. Conversely, RAM is upregulated during T cell activation, leading to questions around the role of RAM in gene regulation during this process (5).

Here we report that during T cell activation, RAM is required for upregulation of RNMT and the gene regulation associated with ribosome production. Deletion of the *Ram* gene results in reduced protein synthesis and reduced proliferation in activated T cells.

Methods & Materials

Mice Animal experiments were performed in accordance with UK Home Office and ARRIVE guidelines. Reviewed by the University of Dundee Welfare and Ethical Use of Animals Committee and the University of Glasgow Animal Welfare and Ethical Review Board. *Ram (Ramac/Fam103a1)* $^{fl/fl}$ mice (loxP sites flanking exon 2 of *Ramac)* were sourced from Taconic Artemis Gmbh. *Rnmt* $^{fl/fl}$ mice with loxP sites flanking exon 3 of *Rnmt* were published previously (5). CD4-Cre (Tg(Cd4-cre)1Cwi mice were published previously (21). Animals used in this study were on a C57BL/6J background. Mice were housed in a pathogen-free environment and kept under standard conditions with a 12-hr day/night cycle with access to food and water ad libitum. Environmental enrichments were added to all cages. Genotyping of ear notches taken at weaning was performed by either the MRC unit genotyping team or Transnetyx. Mice were bred in compliance with EU and Health Products Regulatory Authority standards and used between 8 and 14 weeks old. For all experiments, one mouse represents one biological replicate.

T cell extraction Lymph nodes (inguinal, brachial, axillary, superficial cervical, mesenteric, lumbar, caudal), spleens and thymi were dissected from mice and passed through a 70µm cell strainer (Falcon) to prepare cell suspensions in T cell culture medium: RPMI 1640 medium, Thermo Fisher Scientific) supplemented with 10% heat inactivated Fetal Bovine Serum (FBS) (Thermo Fisher Scientific), 50,000U of Penicillin-Streptomycin (Thermo Fisher Scientific) and 50µM B-mercaptoethanol (Merck). Cells were counted either using the BD FACSVerse (BD Biosciences), Novocyte (Acea Biosciences) or Attune NxT Flow Cytometer (Thermo Fisher Scientific). For this purpose, cells were incubated with labelled antibodies and FC block (anti CD16/32, Biolegend) in Phosphate-buffered Saline (PBS) + 2% FBS. Cells were labelled with 0.1 µg/ml DAPI. Details of all antibodies used in this study in Table S6.

***Ex vivo* activation of CD4 and CD8 T cells** For proliferation analysis, cells isolated from spleens were cultured in T cell culture medium with 0.5ug/ml Ultra-LEAF purified anti-mouse CD3ε antibody (clone 145-2C11, Biolegend), and 0.5ug/ml Ultra-LEAF purified anti-mouse CD28 antibody (clone 37.51, Biolegend). 20 ng/ml interleukin 2 (IL-2, Proleukin, Norvatis) was added on day 2 and 3. CD4 or CD8 T cell numbers and forward scatter (FSC-A) were assessed using a Novocyte flow cytometer (Aceabio) or Attune NxT Flow Cytometer (Thermo Fisher Scientific). CD4 T cells were MACS magnet sorted using a mouse CD4+ T cell Kit (130-104-454; Miltenyi Biotec). Live and T cell numbers and purity (resulting in

minimum 90%) were assessed using a Novocyte flow cytometer (Aceabio). Gating strategies for FACS are presented in supplemental Figures 1-4.

RNA preparation for mass spectrometry and RNA sequencing RNA was extracted using Tri-reagent (Sigma) or Trizol (Thermo Fisher Scientific) and quantified by Nanodrop (Thermo Fisher Scientific) or Qubit™ RNA BR Assay Kit (Thermo Fisher).

CAP-MAP Cap analysis protocol with minimal analyte processing (CAP-MAP) was used to analyse RNA cap structures by Mass Spectrometry (MS) (5, 22).

RNA sequencing analysis *Rnmt* and *Ram* cKO T cells were magnet sorted from mouse lymph nodes using a mouse CD4+ T Cell Isolation Kit (Miltenyi Biotec), then activated for 20 hours on anti-CD3 antibody (5 µg/ml) and anti-CD28 antibody (1 µg/ml) coated plates in T cell medium. CD4 T cell purities were assessed by flow cytometry and were ~98%. Cre recombinase negative littermates (Cre-) were used as controls. RNA was isolated using Tri-reagent (Sigma) and submitted to Genewiz for strand-specific Illumina library preparation using ribosomal RNA depletion and Illumina NovaSeq paired end 150 bp sequencing. Sequence quality was checked using FastQC. Sequences were aligned to mm10 with gencode vM25 basic annotation, and gene count tables generated using STAR version 2.5.2b. Differential gene expression analysis was performed in R with EdgeR using a counts per million (CPM) threshold of 1 in at least three samples. Gene annotations were downloaded using biomaRt, plots drawn using ggplot2 and genes with and FDR below 0.05 in the differential expression analysis were submitted to Webgestalt using Wikipathways for gene set overrepresentation analysis. To assess sRNA (small RNAs) expression, reads were aligned to mm10 using STAR 2.5.2b with filters on multimapping reads removed to avoid losing data on small RNAs contained in repeating genes. Gene counts were recalculated with HTseq such that the primary alignments of multimapping reads were counted then summed read counts for each RFAM sRNA gene family were calculated. Differential expression analysis was repeated using EdgeR including the mRNA read counts to allow read count normalisation and using a cpm threshold of 1 in at least three samples. For splicing analysis, a custom GFF annotation file, including intron and exon locations was generated using a perl script posted on seqanswers (http://seqanswers.com/forums/showthread.php?t=42420) by Alejandro Reyes and then sorted according to strand in R. Exonic and intronic reads were counted using HTSeq, and differential splicing analysis was carried out using DEXseq. Plots were drawn using ggplot2.

Western Blot T cells were lysed in 10 mM Tris HCl pH 7.05; 50 mM NaCl; 30 mM $Na_4P_2O_7$; 50 mM NaF; 10% glycerol; 0.5% triton X-100; 10 mM aprotonin; 1 mM leupeptin; 1 mM pepstatin; 10 mM PI2, 10 mM PI3 and 100 mM DTT on ice and sonicated five times for 30 seconds at medium intensity on Bioruptor (Diagenode). Protein samples from 1-5 $x10^5$ cells were resolved by SDS-PAGE and transferred into PVDF membranes with Tris-glycine buffer (25 mM Tris, 190 mM glycine, 20% methanol). Membranes were incubated with primary antibodies (polyclonal anti-RNMT or anti-RAM antibodies, in house; anti-GAPDH or anti-ACTIN antibodies, Table S6) for two hours at room temperature, followed by incubation with the relevant HRP-conjugated secondary antibodies (Table S6) for one hour at room temperature. Signals were developed using Pierce Super Signal ECL (Thermo Fisher Scientific) and visualised digitally using Fuji Las 4000 (Fujifilm).

Translation assay For assessing the efficiency of translation, *ex vivo* activated T cells from control and *Ram* cKO mice, collected on day 1 and day 2, were incubated with 1 ug/ml Puromycin for 10 min at 37°C in T cell culture medium, stained with Fixable Viability Dye eFluor 780 (eBioscience), fixed with 1% PFA in PBS (Santa Cruz Biotech) on ice, permeabilised and stained using anti-Puromycin antibodies (Millipore) and other surface markers (as above) in saponin buffer (PBS+ 5% FBS + 0.1% saponin).

Statistics The statistical significance of the results presented was calculated using double sided, unpaired Student's t-test. Statistical analysis in bioinformatics described in RNA sequencing analysis.

Results and Discussion

The RNMT cap methyltransferase activator, RAM, is upregulated during T cell activation

We investigated the mechanisms by which gene expression is increased during T cell activation. Following activation of CD4 T cells *ex vivo*, RNMT and its activating subunit RAM were upregulated (Figure 1A). RAM and RNMT were also found to be upregulated on CD4 and CD8 T cells activation in the ImmPRess mass spectrometry data set (23). To study the role of RAM in T cells, we deleted the *Ram* gene (*Ramac*) at the double positive (DP) stage of T cell development. Mice with floxed *Ram* alleles were crossed with mice expressing CD4 promoter-driven Cre recombinase (CD4-Cre) to generate $Ram^{fl/fl}$ CD4-Cre mice (*Ram* cKO, conditional knock-out, Figure 1B, C)(21). *Ram* gene deletion occurs in CD4+ CD8+ DP cells, the developmental precursors of CD4 and CD8 single positive (SP) T cells (Figure 1C). Loss of RAM protein was confirmed in *Ram* cKO CD4 T cells (Figure 1D). In activated *Ram* cKO CD4 T cells there was also decreased RNMT protein, consistent with the dependency of RNMT expression on RAM protein observed in other cell lineages and cell lines (Figure 1D) (15, 19, 24).

Ram is required for T cell development and activation

Ram cKO DP, CD4 SP and CD8 SP thymocytes were similar in number to controls (Figure 2A). In the spleen and peripheral lymph nodes, the number of _Ram_ cKO CD8 T cells was reduced whereas the number of Ram cKO CD4 T cells was unchanged (Figure 2B, C). Previously in _Rnmt_ cKO (_Rnmt_$^{fl/fl}$ CD4-Cre mice), the number of CD8 and CD4 T cells was observed to be reduced in the spleen and lymph nodes, with a greater reduction in CD8 T cells (5). Therefore, deletion of _Rnmt,_ the cap methyltransferase catalytic subunit, has a more severe impact on development than deletion of _Ram,_ the co-factor. In the mesenteric lymph nodes (mLNs), _Ram_ cKO CD4 and CD8 T cells were increased (Figure 2D). Increased T cells in the mLN was also observed in the _Rnmt_ cKO (data not shown). The mechanism behind the increased cellularity of the mLNs is unknown but might involve mild inflammation and increased recruitment of immune cells. Consistent with this, _Rnmt_ cKO and _Ram_ cKO mice occasionally develop anal prolapses (approximately 5% incidence). We speculate that this phenotype may relate to reduced T-regulatory cell function which could reduce tolerance to gut antigens and affect gut epithelial homeostasis (25). The impact of _Ram_ cKO on naïve, central memory, and effector memory CD4 and CD8 T cells was assessed by analysing CD62L and CD44 expression (Figure 2E). Most splenic and lymph node T cells in uninfected mice are expected to have a naïve phenotype and this was the case in both control and _Ram_ cKOs. The proportion of central memory CD4 and CD8 T cells (CD62L high/CD44 high), was lower in _Ram_ cKOs , consistent with decreased numbers of CD4 and CD8 central memory cells in the spleen and peripheral lymph nodes.

Ram is required for the proliferation of activated T cells

Following activation _ex vivo_ by culturing with anti-CD3 and anti-CD28 antibodies, CD4 and CD8 T cells in spleen cell suspensions from control mice proliferated rapidly (Figure 3A, B). _Ram_ cKO CD4 and CD8 T cells failed to proliferate. Activated _Ram_ cKO CD4 T cells had lower forward scatter (FSC-A), than controls, indicating reduced size (Figure 3C). The _Ram_ cKO CD8 T cell FSC was equivalent to controls (Figure 3D). In _Rnmt_ cKO, CD4 and CD8 T cells also had reduced FSC and proliferation, therefore following activation _Ram cKO_ T cells are exhibiting a similar but milder phenotype to _Rnmt_ cKO ((5), data not shown).

Since RAM increases RNMT-dependent m7G cap methylation, we investigated the impact of _Ram_ deletion on RNA cap structures (8, 15, 17). CAP-MAP mass spectrometry was used to quantitate RNA cap structures in CD4 T cells (Figure 4) (22). As previously reported, wild type T cells have a ^{m7}G cap structure

on almost all mRNA (Figure 4A) (5, 22). In *Ram* cKO CD4 T cells, the mature caps $^{m7}GpppC_m$, $^{m7}GpppA_m$, $^{m7}GpppG_m$ were decreased (Figure 4A). Consistent with loss of guanosine cap methylation (^{m7}G) some of the corresponding precursor immature caps, $GpppA_m$, $Gppp^{m6}A_m$, and $Gppp^{m6}A_m$, were increased (Figure 4A). When the initiating transcribed nucleotide was G or A, the corresponding ^{m7}G caps $^{m7}GpppG_m$ and $^{m7}GpppA_m$/$^{m7}Gppp^{m6}A_m$ were reduced by approximately 25% in *Ram* cKO and *Rnmt* cKO CD4 T cells (Figure 4B). When the first transcribed nucleotide was cytosine, the proportion of m7G caps remained high in *Ram* and *Rnmt* cKO CD4 T cells, consistent with $GpppC_m$ and other immature C caps being unstable (Figure 4B). As a consequence, *Ram* cKO T cells had a lower proportion of mRNAs initiating with cytidine (Figure 4C), and a similar observation was made in *Rnmt* cKO (5).

***Ram* controls the expression of mRNA and snoRNA associated with ribosome biogenesis**

Since *Ram* cKO T cells had reduced proliferation, we investigated changes in their transcriptome which may be consistent with this defect. *Ram* cKO CD4 T cells were activated *ex vivo* for 24 hours and the transcriptomes were analysed by RNA sequencing. The sequencing performed here will not distinguish mechanism of gene regulation and whether RAM has a direct or indirect impact, however all genes regulated will potentially contribute to the phenotype observed. Out of 13,140 genes whose RNAs passed detection thresholds, 3,496 were significantly reduced and 3,294 were significantly upregulated in the *Ram* cKO CD4 T cells compared to controls (Figure 5A, Table S1). Consistent with a defect in cell growth and proliferation, gene set overrepresentation analysis indicated that RNAs downregulated in *Ram* cKO CD4 T cells were highly enriched for transcripts encoding ribosomal proteins, with over 80% of genes in this pathway being sensitive to *Ram* deletion (Figure 5B, Table S1). Other downregulated RNAs in the *Ram* cKO T cells belonged to gene families associated with metabolism, amino acid biosynthesis pathways, TCA cycle and DNA replication pathways. Within the group of upregulated genes in the *Ram* cKO cells, there were genes encoding proteins involved in signalling or apoptosis (Figure 5C, Table S1).

Since deletion of *Ram* in T cells was having a similar but milder phenotype to that observed on deletion of *Rnmt,* we investigated if a subset of *Rnmt* dependent genes is also *Ram* dependent. The regulation of RNAs in *Ram* cKO and *Rnmt* cKO CD4 T cells had a high correlation (Figure 5 D-F, Table S2 and S5). The transcripts of 2,907 genes were repressed in both *Ram* cKO and *Rnmt* cKO CD4 T cells, 589 genes were repressed only in *Ram* cKO and 607 were repressed only in *Rnmt* cKO. 2,668 genes were increased in both *Ram* cKO and *Rnmt* cKO CD4 T cells, 626 genes were increased in *Ram* cKO only and 599 genes were increased in *Rnmt* cKO only. Notably, no genes were significantly changed in the opposite

directions in *Rnmt* and *Ram* cKO CD4 T cells. Of the genes that were responsive to both *Rnmt* and *Ram* cKOs, there was a trend towards larger fold changes in the *Rnmt* cKO.

All RNA pol II transcripts have the potential to initially receive a ^{m7}G cap, including the small nuclear RNAs (snRNAs), small nucleolar RNAs (snoRNAs) and small Cajal bodies-specific RNAs (scaRNAs) (26, 27). The cap of most snoRNAs and scaRNAs is removed as they are processed from introns or precursor long non-coding RNAs. When the cap is retained on small RNAs, they receive additional cap modifications. The caps on small RNA caps are methylated by RNMT and we previously confirmed that their expression is RNMT dependent in T cells (5). Transcript sequencing indicated that 93 snoRNAs were decreased out of 176 detected in *Ram* cKO CD4 T cells, compared to controls (Figure 6A, table S3). Similarly, in *Rnmt* cKO, 88 snoRNAs were repressed (Table S4). In contrast, many scaRNAs were upregulated in *Ram* cKO and *Rnmt* cKO T cells when compared to control (8 and 6 scaRNAs respectively, out of 16 detected) (Figure 6A, B, Table S3 and 4). snRNAs were mildly impacted; out of 9 detected, 1 was increase and 1 was decreased in *Ram* cKO T cells and 4 were increased in *Rnmt* cKO activated CD4 T cells (Figure 6A, B, Table S3 and s4).

Although changes in snRNA were minimal in *Ram* cKO, the ^{m7}G cap can also influence splicing by recruiting the Cap Binding Complex (CBC), which aids first intron removal (28, 29). A defect in splicing of the first intron was observed in the transcriptome analysis in activated *Ram* cKO CD4 T cells (Figure 6C), similarly to the defect observed in activated *Rnmt* cKO CD4 T cells (Figure 6D).

Ram is required for protein synthesis in activated T cells

To investigate the functional consequences of *Ram* KO, we analysed translation rates using puromycin incorporation into nascent peptides. In *Ram* cKO CD4 T cells, puromycin incorporation was reduced indicating reduced translation, consistent with reduced expression of ribosomal proteins and ribosome biogenesis factors (Figure 6E). In *Ram* cKO CD4 T cells, total RNA per cell was reduced, the majority of which is ribosomal RNA (Figure 6F). Reduced ribosomal RNA is consistent with reduced expression of TAF1D, a RNAPI component, reduced UTP14a, a component of the U3 snoRNP which mediates rRNA cleavage and reduced NPM1 a ribosome biogenesis factor.

In summary, regulation of gene expression is critical to T cell function; increasing cellular protein content during activation and proliferation, and reshaping the proteome during differentiation into distinct T cell lineages. RNA cap formation has important roles in RNA expression, stability, processing and translation. Here we describe that RAM, the co-factor for the N-7 guanosine cap methyltransferase RNMT is

upregulated during T cell activation and is required for RNMT expression and function in methylating the RNA cap guanosine. On *Ram* gene deletion, T cells fail to proliferate following activation. Consistent with this defect in growth and proliferation the RNAs repressed in *Ram* cKO are members of the ribosomal gene family and the snoRNAs which mediate ribosomal RNA processing. In addition to RAM, RNMT also interacts with eIF4E and eIF4E impacts on RNA cap formation. The RNMT-eIF4E interaction may have roles during T cell activation, particularly in RNA export and translation initiation (30, 31). The role of the other capping enzymes in T cell activation is yet to be determined.

Acknowledgements

We would like to thank members of the Cowling, Cantrell and Blyth labs for useful discussions, the Tayside Centre for Genomic Analysis, the Dundee University and Beatson Institute Biological Resource Units, Mass spectrometry facilities and Flow Cytometry facilities.

Ethical approval

Animal experiments were performed in accordance with UK Home Office and ARRIVE guidelines. Reviewed by the University of Dundee Welfare and Ethical Use of Animals Committee and the University of Glasgow Animal Welfare and Ethical Review Board.

Funding

This work was supported by Cancer Research UK core funding to the CRUK Beatson Institute (A31287), by the European Research Council (ERC) under the European Union's Horizon 2020 research and innovation programme [769080]; a Wellcome Trust Investigator Award (219416/Z/19/Z) to V.H.C, and a Royal Society Wolfson Research Merit Award [WRM\R1\180008]

Conflicts of interest

The authors declare no conflicts of interest.

Data availability

RNA sequencing data is present in the GEO data series: GSE198541

Author Contributions

All authors were involved in project conceptualisation, investigation, analysis and writing.

Figure legends

Figure 1. RAM and RNMT are upregulated following T cell activation

(A) Western blot analysis of RAM and RNMT protein levels in naïve (day 0), and *ex vivo* activated (day 1 and 2) CD4 T cells. ACTIN was used as loading control. Data generated from cells of one mouse and is representative of data from 3 mice. (B) Schematic of *Ram* cKO strategy. (C) The *Ram* cKO T cell model: progenitor and mature T cell populations and *ex vivo* activation protocol are depicted. *Ram* deletion is in the double positive (DP; CD4+ CD8+) thymocytes. (D) Western blot analysis of RAM and RNMT protein levels in control (*Ram* $^{fl/fl}$) and *Ram* cKO activated CD4 T cells. Sample in each lane generated from cells of one mouse. RNMT immunoprecipiates (+) from mouse brain lysates and (-) from liver lysates were used to verify migration of RAM. GAPDH was used as loading control. A star indicates the RAM band.

Figure 2. *Ram* deletion results in a reduction in CD8 T cells

(A) Number of CD4 and CD8 double negative (DN), double positive (DP) and single positive T cells in thymus in control (*Ram*$^{fl/fl}$, n=5) and *Ram* cKO (n=5) mice. Representative FACS plot, right panel, including % in each gate. Number of CD4 and CD8 T cells in (B) spleen (control (n=5) and *Ram* cKO (n=4) mice), (C) peripheral lymph nodes (pLNs) (control (n=5) and *Ram* cKO (n=5) mice) and (D) mesenteric lymph nodes (mLNs) (control (n=4) and *Ram* cKO (n=5) mice). (E) Percentage of CD4 and CD8 CD62L high, CD62L/CD44 high and CD62L low T cells in spleen (top panel, control (n=5) and *Ram* cKO (n=5) mice), peripheral lymph nodes (pLNs, middle panel, control (n=5) and *Ram* cKO (n=5) mice), and mesenteric lymph nodes (mLNs, bottom panel, control (n=5) and *Ram* cKO (n=4) mice). Dots indicate biological replicates, lines indicate means, p values from Student's t test. Gating strategies are depicted in Supplementary Figure 1 and 2.

Figure 3. Activated Ram cKO CD4 and CD8 T cells have a proliferation defect

Splenocytes from control (*Ram*$^{fl/fl}$) (n=3) and *Ram* cKO mice (n=3) were activated *ex vivo* and cultured. Number of cells was determined: (A) CD4 T cells and (B) CD8 T cells. Forward scatter (FSC-A) was measured on Day 1 and 2 in (C) CD4 T cells, (D) CD8 T cells. Representative histograms left panels. MFI plots, right panels (n=4). Dots indicate biological replicates, lines indicate means, p values from Student's t test. Gating strategies are depicted in Supplementary Figure 2 and 3.

Figure 4. Ram cKO CD4 T cells have reduced ^{m7}G-capped RNA

CD4 T cells were purified from control (n=3), *Ram* cKO (n=3) and *Rnmt* cKO (n=3) mice and activated *ex vivo* for 26 hours. (A) CAP-MAP quantitation of cap structures in control and *Ram* cKO CD4 T cell mRNA. Note C cap detection failed in one *Ram* cKO replicate. (B) Proportion of ^{m7}G-capped mRNAs initiating

with guanosine (G), adenine (A) or cytosine in *Ram* cKO and *Rnmt* cKO CD4 T cells. (D) Proportion of capped mRNAs initiating with guanosine (G), adenine (A) or cytosine (C) in control and *Ram* cKO CD4 T cells. Dots show biological replicates, bars indicate mean, p values from Student's t test.

Figure 5. A comparison of the RNMT and RAM regulated transcriptomes

(A) MA plot of RNA expression in control (*Ram fl/fl,* n=3) and *Ram* cKO (n=3) activated CD4 T cells. Dots represent genes. Reads per million mapped reads (RPM) on x-axis. Control and *Ram* cKO samples were compared using EdgeR exact test and adjusted p value used. Pathway analyses (FDR<30%) of significantly (B) downregulated or (C) upregulated *Ram* cKO target RNAs (adjusted p value <0.05). (D) Comparison of RNA level changes in *Ram* cKO (n=3) and *Rnmt* cKO (n=3) activated CD4 T cells. Equivalently regulated genes, pink; regulated in *Ram* cKO only, green; regulated in *Rnmt* cKO only, blue. Pathway analyses of *Ram* cKO and *Rnmt* cKO shared target RNAs (FDR<30%), (E) downregulated or (F) upregulated (adjusted p value <0.05).

Figure 6. RAM is required for efficient translation following T cell activation

(A) Small RNA levels in *Ram* cKO (n = 3) and control ($Ram^{fl/fl}$, n=3) activated CD4 T cells, grouped by RFAM family. Small nuclear RNAs (snRNAs), green; small nucleolar RNAs (snoRNAs), pink; small Cajal-body specific RNAs (scaRNAs), blue. Filled dots, adjusted p value <0.05. (B) Comparison of small RNA level changes in *Ram* cKO and *Rnmt* cKO CD4 T cells compared to controls ($Ram^{fl/fl}$, $Rnmt^{fl/fl}$, respectively). (C-D) Splicing analysis in activated CD4 T cells. Reads aligning to exons and introns were normalised to the total reads for the transcript and read densities for each transcript were compared between controls and (C) *Ram* cKO and (D) *Rnmt* cKO. Violin plots represent the frequency density. Box plots show median, upper and lower quartiles. Whiskers, 1.5 X interquartile range. (E) CD4 T cells were activated *ex vivo* and translation rates determined using puromycin incorporation into nascent peptides. Control (n=3) and *Ram* cKO (n=4). Cells incubated without puromycin were used for a baseline signal. (F) RNA yield from 10^6 control and *Ram* cKO CD4 T cells activated *ex vivo* for 24hrs (n=3). Dots show biological replicates, bars indicate mean, p values from Student's t test. Gating strategy is depicted in Supplementary Figure 6.

References

1. Wolf T, Jin W, Zoppi G, Vogel IA, Akhmedov M, Bleck CKE, et al. Dynamics in protein translation sustaining T cell preparedness. Nat Immunol. 2020;21(8):927-37. 10.1038/s41590-020-0714-5
2. Howden AJM, Hukelmann JL, Brenes A, Spinelli L, Sinclair LV, Lamond AI, et al. Quantitative analysis of T cell proteomes and environmental sensors during T cell differentiation. Nat Immunol. 2019;20(11):1542-54. 10.1038/s41590-019-0495-x
3. Marchingo JM, Cantrell DA. Protein synthesis, degradation, and energy metabolism in T cell immunity. Cell Mol Immunol. 2022;19(3):303-15. 10.1038/s41423-021-00792-8
4. Turner M. Regulation and function of poised mRNAs in lymphocytes. Bioessays. 2023;45(5):e2200236. 10.1002/bies.202200236
5. Galloway A, Kaskar A, Ditsova D, Atrih A, Yoshikawa H, Gomez-Moreira C, et al. Upregulation of RNA cap methyltransferase RNMT drives ribosome biogenesis during T cell activation. Nucleic Acids Res. 2021;49(12):6722-38. 10.1093/nar/gkab465
6. Galloway A, Cowling VH. mRNA cap regulation in mammalian cell function and fate. Biochim Biophys Acta Gene Regul Mech. 2019;1862(3):270-9. 10.1016/j.bbagrm.2018.09.011
7. Pelletier J, Schmeing TM, Sonenberg N. The multifaceted eukaryotic cap structure. Wiley Interdiscip Rev RNA. 2021;12(2):e1636. 10.1002/wrna.1636
8. Varshney D, Lombardi O, Schweikert G, Dunn S, Suska O, Cowling VH. mRNA Cap Methyltransferase, RNMT-RAM, Promotes RNA Pol II-Dependent Transcription. Cell Rep. 2018;23(5):1530-42. 10.1016/j.celrep.2018.04.004
9. Trotman JB, Schoenberg DR. A recap of RNA recapping. Wiley Interdiscip Rev RNA. 2019;10(1):e1504. 10.1002/wrna.1504
10. Fonseca BD, Lahr RM, Damgaard CK, Alain T, Berman AJ. LARP1 on TOP of ribosome production. Wiley Interdiscip Rev RNA. 2018:e1480. 10.1002/wrna.1480
11. Berman AJ, Thoreen CC, Dedeic Z, Chettle J, Roux PP, Blagden SP. Controversies around the function of LARP1. RNA Biol. 2021;18(2):207-17. 10.1080/15476286.2020.1733787
12. Lahr RM, Mack SM, Heroux A, Blagden SP, Bousquet-Antonelli C, Deragon JM, et al. The La-related protein 1-specific domain repurposes HEAT-like repeats to directly bind a 5'TOP sequence. Nucleic Acids Res. 2015;43(16):8077-88. 10.1093/nar/gkv748
13. Lahr RM, Fonseca BD, Ciotti GE, Al-Ashtal HA, Jia JJ, Niklaus MR, et al. La-related protein 1 (LARP1) binds the mRNA cap, blocking eIF4F assembly on TOP mRNAs. Elife. 2017;6. 10.7554/eLife.24146
14. Cassidy KC, Lahr RM, Kaminsky JC, Mack S, Fonseca BD, Das SR, et al. Capturing the Mechanism Underlying TOP mRNA Binding to LARP1. Structure. 2019;27(12):1771-81 e5. 10.1016/j.str.2019.10.006
15. Gonatopoulos-Pournatzis T, Dunn S, Bounds R, Cowling VH. RAM/Fam103a1 Is Required for mRNA Cap Methylation. Molecular cell. 2011;44(4):585-96. 10.1016/j.molcel.2011.08.041
16. Bueren-Calabuig JA, M B, Cowling VH, Pisliakov AV. Mechanism of allosteric activation of human mRNA cap methyltransferase (RNMT) by RAM: insights from accelerated molecular dynamics simulations. Nucleic Acids Res. 2019;47(16):8675-92. 10.1093/nar/gkz613

17. Varshney D, Petit AP, Bueren-Calabuig JA, Jansen C, Fletcher DA, Peggie M, et al. Molecular basis of RNA guanine-7 methyltransferase (RNMT) activation by RAM. Nucleic Acids Res. 2016;44(21):10423-36. 10.1093/nar/gkw637
18. Gonatopoulos-Pournatzis T, Cowling VH. RAM function is dependent on Kapbeta2-mediated nuclear entry. The Biochemical journal. 2014;457(3):473-84. 10.1042/BJ20131359
19. Grasso L, Suska O, Davidson L, Gonatopoulos-Pournatzis T, Williamson R, Wasmus L, et al. mRNA Cap Methylation in Pluripotency and Differentiation. Cell reports. 2016;16(5):1352-65. 10.1016/j.celrep.2016.06.089
20. Liang S, Almohammed R, Cowling VH. The RNA cap methyltransferases RNMT and CMTR1 co-ordinate gene expression during neural differentiation. Biochem Soc Trans. 2023. 10.1042/BST20221154
21. Lee PP, Fitzpatrick DR, Beard C, Jessup HK, Lehar S, Makar KW, et al. A critical role for Dnmt1 and DNA methylation in T cell development, function, and survival. Immunity. 2001;15(5):763-74. 10.1016/s1074-7613(01)00227-8
22. Galloway A, Atrih A, Grzela R, Darzynkiewicz E, Ferguson MAJ, Cowling VH. CAP-MAP: cap analysis protocol with minimal analyte processing, a rapid and sensitive approach to analysing mRNA cap structures. Open Biol. 2020;10(2):190306. 10.1098/rsob.190306
23. Brenes AJ, Lamond AI, Cantrell DA. The Immunological Proteome Resource. Nat Immunol. 2023;24(5):731. 10.1038/s41590-023-01483-4
24. Dunn S, Lombardi O, Lukoszek R, Cowling VH. Oncogenic PIK3CA mutations increase dependency on the mRNA cap methyltransferase, RNMT, in breast cancer cells. Open Biol. 2019;9(4):190052. 10.1098/rsob.190052
25. Cosovanu C, Neumann C. The Many Functions of Foxp3(+) Regulatory T Cells in the Intestine. Front Immunol. 2020;11:600973. 10.3389/fimmu.2020.600973
26. Cao T, Rajasingh S, Samanta S, Dawn B, Bittel DC, Rajasingh J. Biology and clinical relevance of noncoding sno/scaRNAs. Trends Cardiovasc Med. 2018;28(2):81-90. 10.1016/j.tcm.2017.08.002
27. Wilkinson ME, Charenton C, Nagai K. RNA Splicing by the Spliceosome. Annu Rev Biochem. 2020;89:359-88. 10.1146/annurev-biochem-091719-064225
28. Gonatopoulos-Pournatzis T, Cowling VH. The Cap Binding Complex. The Biochemical journal. 2014;457(Part 2):231-42. 10.1042/BJ20131214
29. Rambout X, Maquat LE. The nuclear cap-binding complex as choreographer of gene transcription and pre-mRNA processing. Genes Dev. 2020;34(17-18):1113-27. 10.1101/gad.339986.120
30. Culjkovic-Kraljacic B, Skrabanek L, Revuelta MV, Gasiorek J, Cowling VH, Cerchietti L, et al. The eukaryotic translation initiation factor eIF4E elevates steady-state m(7)G capping of coding and noncoding transcripts. Proc Natl Acad Sci U S A. 2020;117(43):26773-83. 10.1073/pnas.2002360117
31. Osborne MJ, Volpon L, Memarpoor-Yazdi M, Pillay S, Thambipillai A, Czarnota S, et al. Identification and Characterization of the Interaction Between the Methyl-7-Guanosine Cap Maturation Enzyme RNMT and the Cap-Binding Protein eIF4E. J Mol Biol. 2022;434(5):167451. 10.1016/j.jmb.2022.167451

Figure 1

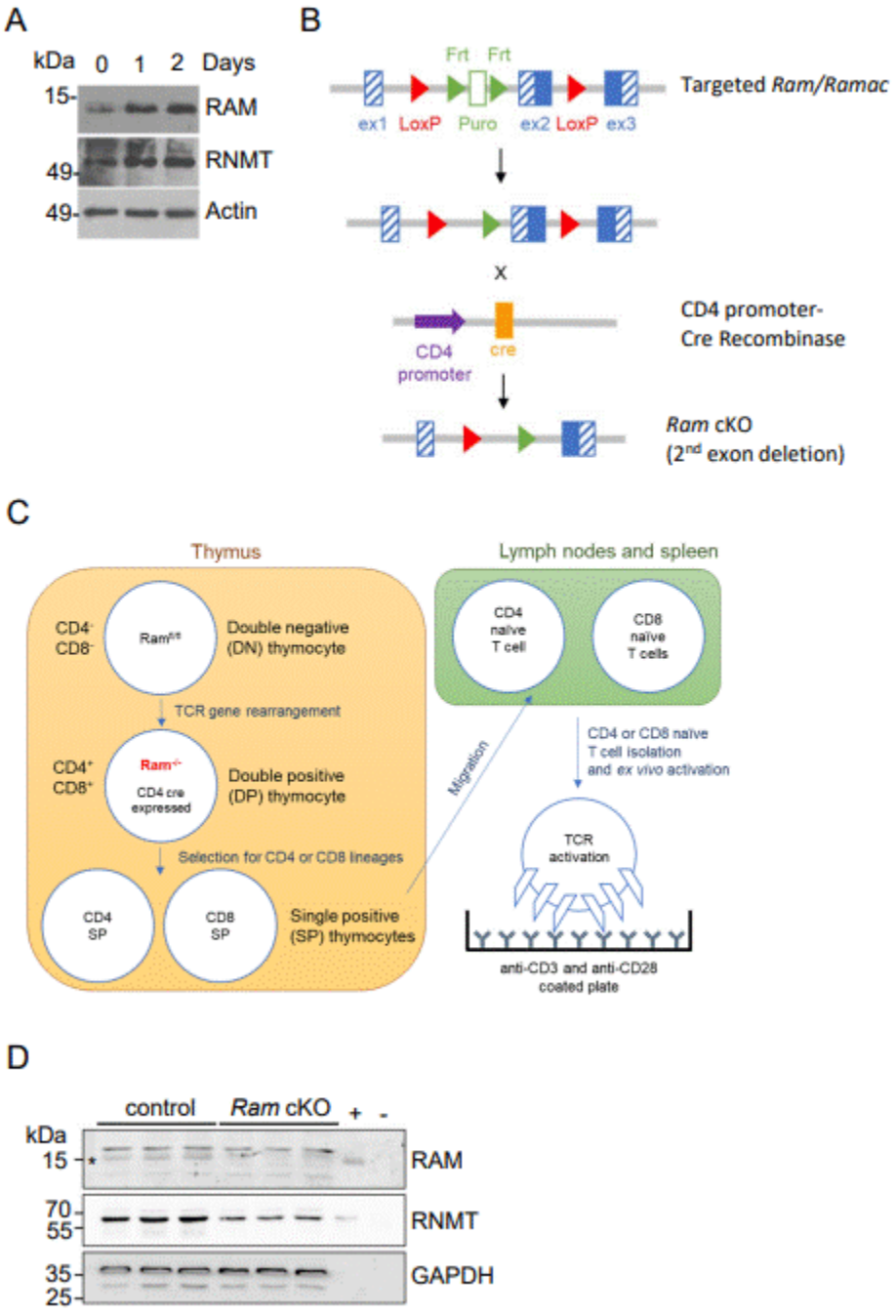

Figure 2

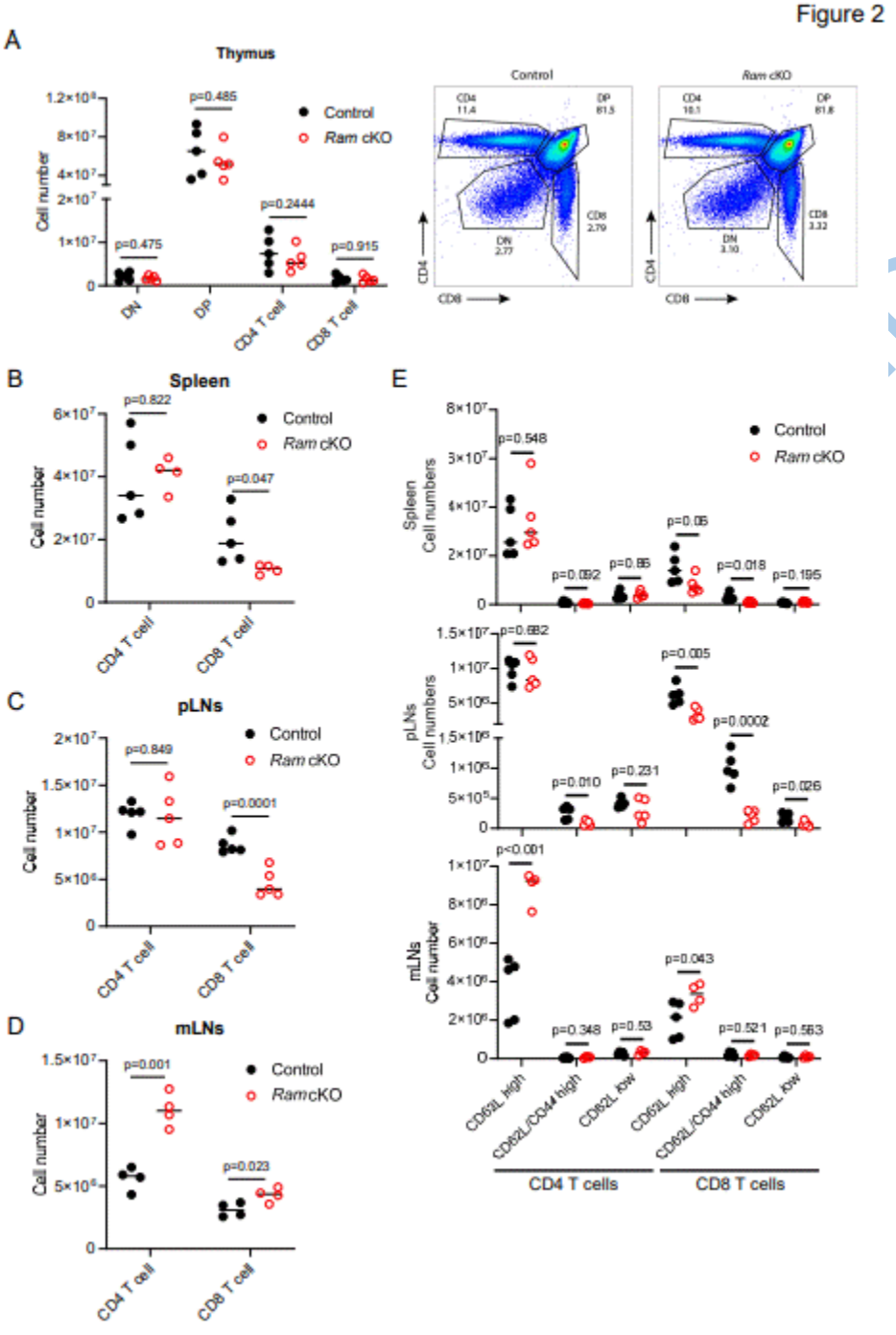

Figure 3

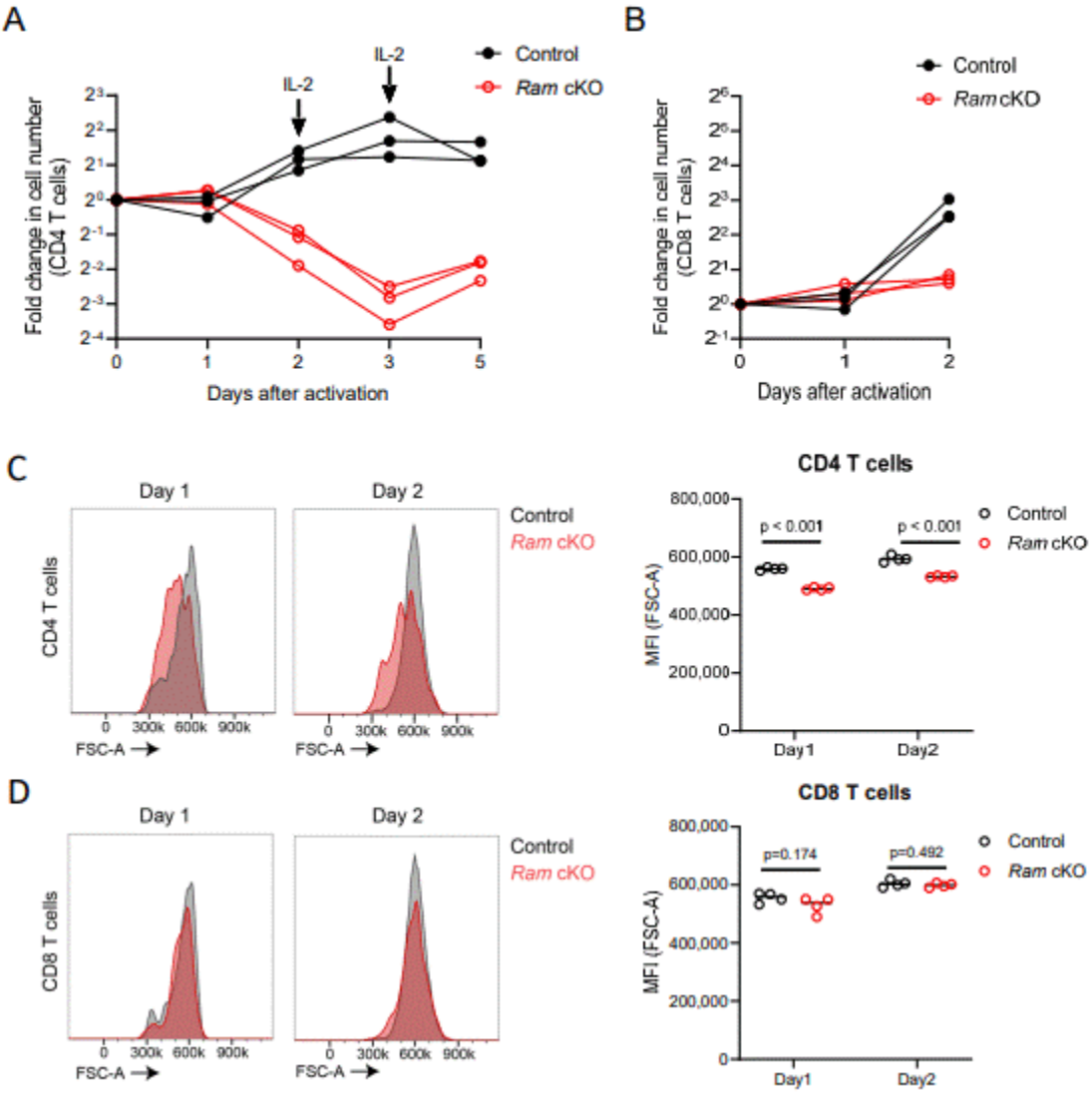

Figure 4

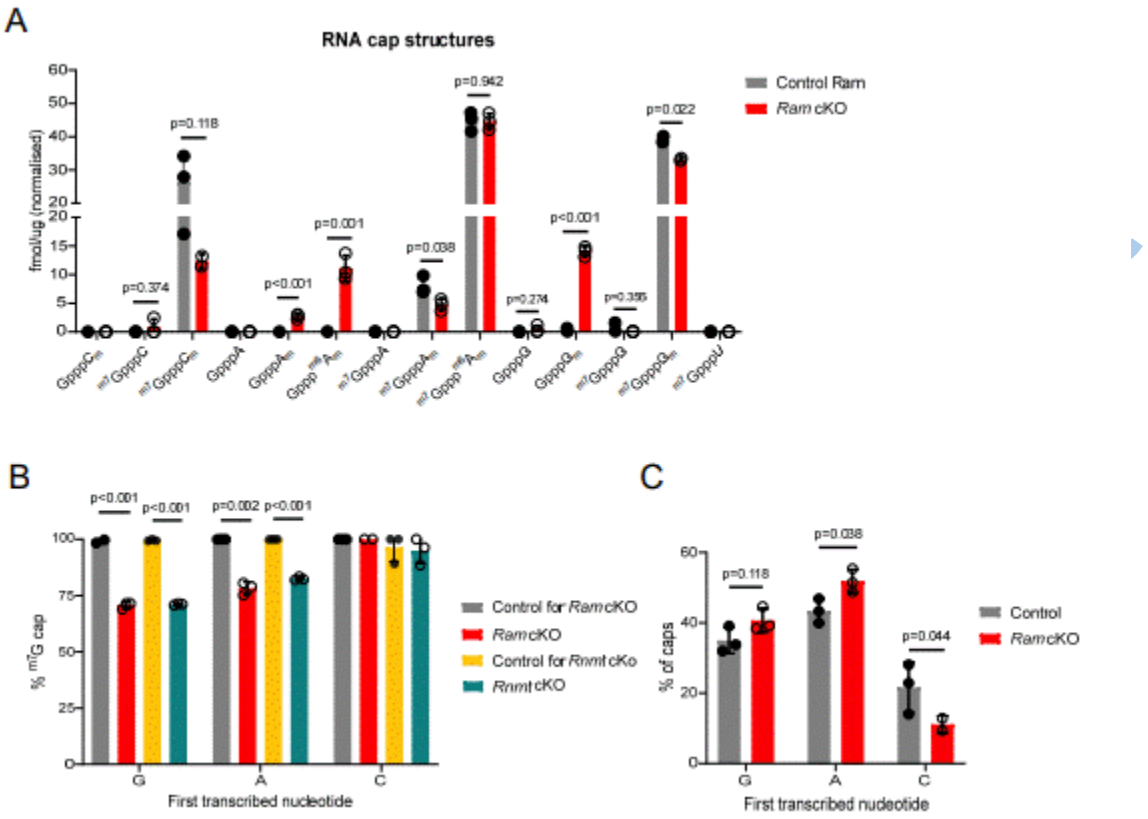

Figure 5

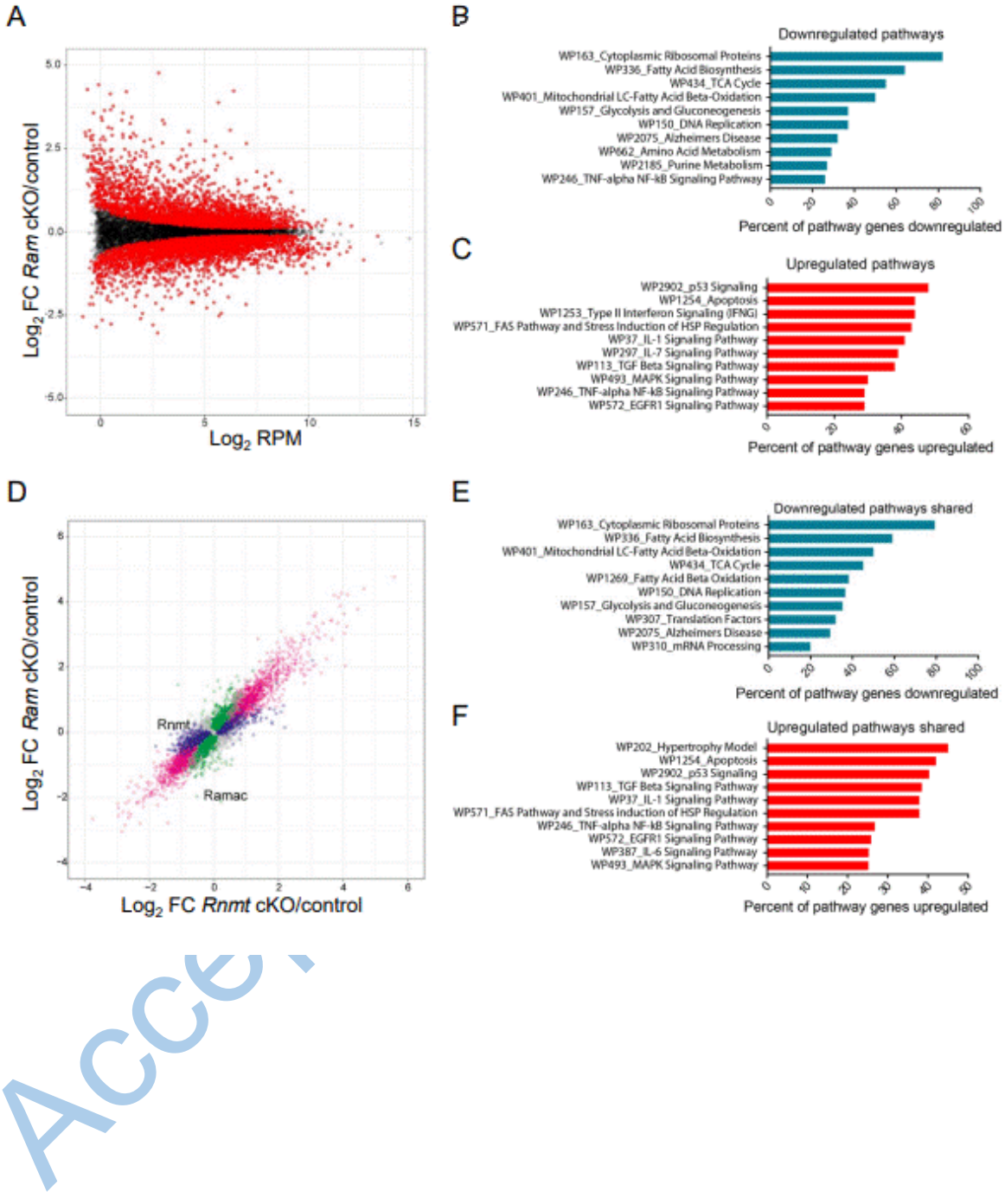

Figure 6